

Hadron collider signatures for new interactions of top and bottom quarksT. Han,¹ G. Valencia,² and Yili Wang^{2,*}¹*Department of Physics, University of Wisconsin, Madison, Wisconsin 53706, USA
and Institute of Theoretical Physics, Academia Sinica, Beijing 100080, China*²*Department of Physics, Iowa State University, Ames, Iowa 50011, USA*

(Received 12 May 2004; published 17 August 2004)

One of the main goals for hadron colliders is the study of the properties of the third generation quarks. We study the signatures for new TeV resonances that couple to top or bottom quarks both at the Tevatron Run II and at the CERN LHC. We find that in the simplest production processes of Drell-Yan type at the Tevatron, the signals are overwhelmed by QCD backgrounds. We also find that it is possible to study these resonances when they are produced in association with a pair of heavy quarks or in association with a single top at the LHC. In particular, with an integrated luminosity of 300 fb^{-1} at the LHC, it is possible to probe resonance masses up to around 2 TeV.

DOI: 10.1103/PhysRevD.70.034002

PACS number(s): 13.85.Qk, 12.60.Fr, 13.38.Dg, 14.80.Bn

I. INTRODUCTION

A major goal for the Fermilab Tevatron and the CERN Large Hadron Collider (LHC) is the detailed study of the properties of the top quark. In particular they should establish whether the third family behaves like the first two, or whether it is subject to new interactions. The interactions of the third family have been studied indirectly in many low energy processes such as rare kaon and B meson decays with no firm evidence for physics beyond the standard model. There are, however, certain inconsistencies [1] associated with the forward-backward asymmetry A_{FB}^b measured at the CERN e^+e^- collider LEP that hint at a potential problem. In any case it is highly desirable to pursue a direct study of the couplings of the top quark in colliders. With this in mind, and motivated by the possibility that the top quark plays a special role in the breaking of electroweak symmetry [2], we have previously studied the signals for a new resonance in the process $W_L W_L \rightarrow t\bar{t}$ [3].

A different type of signal occurs if the new resonances couple strongly to the third generation of quarks but not necessarily to the W and Z gauge bosons. In this paper we study the signatures for this type of new physics at the Tevatron and at the LHC. We first discuss the cases of a vector and a scalar resonance (generically denoted by R) produced in the s -channel processes $q\bar{q} \rightarrow R \rightarrow b\bar{b}$ or $t\bar{t}$. In these processes the QCD backgrounds are large and we apply known techniques to reduce these backgrounds. We then consider the production of the new resonances in association with a $b\bar{b}$ or $t\bar{t}$ pair through processes such as $gg \rightarrow R t\bar{t} \rightarrow b\bar{b} t\bar{t}$ or $t\bar{t} t\bar{t}$. These processes are higher order corrections to the s -channel production and therefore have a significantly smaller cross section. However, their unique topology permits a much better control of the QCD background and we find that they yield potentially observable signals.

In our study of the process $W_L W_L \rightarrow t\bar{t}$ [3] we used

model-independent (but nonrenormalizable) parametrizations for the couplings of the new resonances to the b and t quarks. We found that if these resonances were responsible for electroweak symmetry breaking they were typically very broad when they were as heavy as a few TeV. In order to parametrize new resonances that are heavy and narrow, we argued in Ref. [3] that we had to consider models with more than one new resonance at a time. In this paper we adopt this scenario and do not require that our resonances be responsible for electroweak symmetry breaking. We say nothing of their couplings to W and Z gauge bosons but simply assume that they provide negligible contributions to their widths. A prototype for a vector resonance with such behavior—no coupling to the W and Z gauge bosons; very weak coupling to the first two generations of fermions; and large coupling to b and t quarks—is provided by the Z' boson from Ref. [4]. For definiteness we will have this particle in mind as our vector resonance. We can regard this as a fairly general parametrization of a new vector resonance with arbitrary couplings to b and t if we abandon renormalizability and treat the resonance couplings as an effective theory, in the spirit of Ref. [3]. For the case of a scalar resonance we use the simple parametrization of the $S b\bar{b}$ and $S t\bar{t}$ couplings that we used in Ref. [3] but we assume a negligible width $\Gamma(S \rightarrow WW)$. The possibility of nonstandard couplings for the top quark has been discussed extensively in the literature in the context of anomalous couplings [5]. Some generic models of vector resonances coupled to the top quark strongly are studied in Ref. [6]. By adding new resonances as explicit degrees of freedom to the effective theory, one is able to study potential nonstandard couplings in a larger energy domain.

II. MODEL FOR NEW STRONGLY INTERACTING RESONANCES**A. Vector resonance**

We begin by discussing our parametrization for the new vector resonance. Effective interactions between the standard model (SM) gauge bosons and fermions and new vector resonances have been described in the literature [7]. We are

*Electronic address: than@pheno.physics.wisc.edu;
valencia@iastate.edu; yiliwa@iastate.edu

interested in new interactions of b and t quarks to new heavy resonances that are sufficiently narrow to be described by a Breit-Wigner shape. One way to accomplish this within the effective Lagrangian framework is to have more than one resonance, as we discussed in Ref. [3]. Here we assume that this is the case, and that the resonance under study has negligible couplings to electroweak gauge bosons. An alternative way to obtain such a resonance is to consider extended gauge sectors. Our goal in this paper is to investigate the extent to which hadron colliders are sensitive to new strong interactions of the top quark regardless of the origin of the new interactions. We thus proceed with the following effective Lagrangian coupling a spin one field to the top and bottom quarks:

$$\mathcal{L} = -\Psi \gamma^\mu (g_V + g_A \gamma_5) \tau_i \Psi V_\mu^i. \quad (1)$$

Vector resonances introduced in this manner occur in the Breaking Electroweak Symmetry Strongly (BESS) model, for example [7]. They have universal couplings to fermions that arise from mixing between the new vectors and the W and Z bosons. In addition there can be nonuniversal direct couplings. We are interested only in the latter in the form of large new couplings to the b and t quarks because universal couplings are severely constrained by low energy observables. In fact, the most stringent constraints on the couplings in Eq. (1) were found in Ref. [3] to arise from mixing between the new V and the W and Z bosons. A direct study of these couplings at high energy will therefore be most relevant for the case of negligible mixing and we concentrate on this case.

In hadron colliders, however, light quark annihilation represents a significant production source for new vector resonances even if they couple predominantly to b and t quarks. This is an unfortunate complication because it forces us to commit to a specific model where the relative couplings between the new vectors and the heavy and light quarks are known. To keep our study as model independent as possible we will illustrate our results for parameters that make the contributions of the light quark annihilation mechanism to resonance production small. We will also compare with a scalar resonance in which we assume no couplings to light fermions exist. For definiteness we will use the Z' model of Ref. [4] in the limit of no V - Z mixing. There exist very tight constraints on the flavor changing neutral currents that appear in this model [4] and, therefore our starting point in this paper will be the flavor diagonal interaction in the quark mass eigenstate basis,

$$\begin{aligned} \mathcal{L} = & \frac{g}{2} \tan \theta_W \tan \theta_R \left(\frac{1}{3} \bar{q}_L \gamma^\mu q_L + \frac{4}{3} \bar{u}_{Ri} \gamma^\mu u_{Ri} - \frac{2}{3} \bar{d}_{Ri} \gamma^\mu d_{Ri} \right) V_\mu \\ & - \frac{g}{2} \tan \theta_W (\tan \theta_R + \cot \theta_R) (\bar{t}_R \gamma^\mu t_R - \bar{b}_R \gamma^\mu b_R) V_\mu. \quad (2) \end{aligned}$$

In this expression g is the standard model $SU(2)_L$ gauge coupling, θ_W is the usual weak mixing angle, and θ_R is a new parameter. Also, q_L is summed over the SM quarks, and repeated indices are summed over the three generations.

With large $\cot \theta_R$, this model provides a specific example of a new vector resonance with couplings to b and t quarks that are significantly enhanced with respect to couplings to the light fermions. In the limit of large $\cot \theta_R$ these couplings are purely right-handed, with

$$g_A = g_V = \frac{g}{4} \tan \theta_W \cot \theta_R. \quad (3)$$

We have checked numerically that the signals discussed in this paper would be very similar if we had left-handed couplings instead.

The resonance width into $b\bar{b}$ or $t\bar{t}$ pairs is¹

$$\begin{aligned} \Gamma(V \rightarrow f\bar{f}) &= \frac{M_V}{2\pi} g_V^2 \left(1 - 4 \frac{m_f^2}{M_V^2} \right)^{1/2} \left(1 - \frac{m_f^2}{M_V^2} \right) \\ &\approx 63 \left(\frac{g_V}{0.63} \right)^2 \left(\frac{M_V}{1000 \text{ GeV}} \right) \text{ GeV}, \text{ for } M_V \gg m_f. \quad (4) \end{aligned}$$

Requiring the new interaction to remain perturbative leads to the theoretical constraint $\cot \theta_R < 20$, equivalently $g_V < 1.8$. Partial wave unitarity requirements do not improve this bound. For illustration purposes, throughout the paper, we will present numerical results with

$$g_V = 0.63 \Leftrightarrow \cot \theta_R = 7. \quad (6)$$

With this choice the couplings of V to b and t are about 50 times larger than the couplings to the light quarks. At the same time the resonance remains narrow, with $\Gamma_V/M_V \sim 0.12$. Notice that the value $g_V \sim 0.63$ is about four times larger than the largest value we considered in Ref. [3]. In that case we were constrained by low energy bounds on V - W mixing, whereas here we consider the case where that mixing is independent of the coupling g_V and effectively remove the constraints.

The relative branching fraction for the decays of the V into $b\bar{b}$ and $t\bar{t}$ is governed simply by kinematics,

$$\frac{\Gamma(V \rightarrow t\bar{t})}{\Gamma(V \rightarrow b\bar{b})} = \left(\frac{M_V^2 - 4m_t^2}{M_V^2 - 4m_b^2} \right)^{1/2} \left(\frac{M_V^2 - m_t^2}{M_V^2 - m_b^2} \right). \quad (7)$$

For small M_V , $\Gamma(V \rightarrow b\bar{b})$ is much larger than $\Gamma(V \rightarrow t\bar{t})$. As M_V nears 500 GeV, $\Gamma(V \rightarrow t\bar{t})$ is only about 62% of $\Gamma(V \rightarrow b\bar{b})$ and increases to 90% when M_V is near 1 TeV.

B. Scalar resonance

We next consider the effective interaction between the third generation quarks and a new scalar resonance. In this case we will use a very simple (nonrenormalizable) param-

¹In Ref. [3] we used an equation for this width that has a typographical error. Numerically it does not affect our conclusions in those papers because it only affects terms that are suppressed by m_i^2/M_R^2 and we considered large resonance masses.

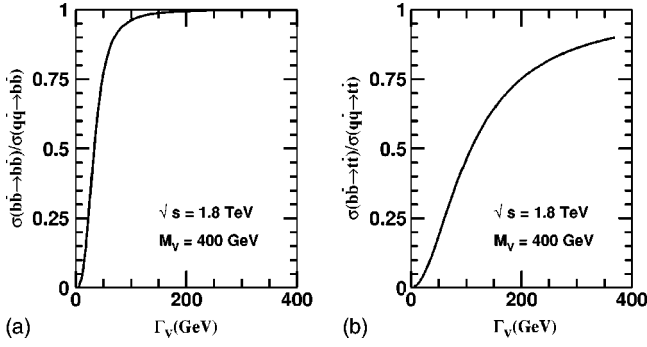


FIG. 1. Relative contributions (a) to $pp\bar{\rightarrow}b\bar{b}X$ and (b) to $t\bar{t}X$ from $b\bar{b}\rightarrow b\bar{b}(t\bar{t})$ and $q\bar{q}\rightarrow b\bar{b}(t\bar{t})$ processes at the Tevatron for $M_V=400$ GeV as a function of Γ_V .

erization for the new interactions, and assume that the couplings of the scalar to the light fermions are completely negligible. We write

$$\mathcal{L} = -\frac{m_t}{v} S(\kappa_b \bar{b}b + \kappa_t \bar{t}t). \quad (8)$$

This form allows us to parametrize simultaneously the cases where either the b quark or the t quark or both have enhanced couplings to the new scalar. Examples where the b quark coupling (rather than the t quark coupling) to a scalar is enhanced occur frequently in multi-Higgs models with large $\tan\beta$. We will assume in this study that the scalar width is dominated by its decay into b and t pairs and that it receives a negligible contribution from decay into W and Z pairs. This corresponds to taking $g_S \sim 0$ in the models discussed in Ref. [3] and therefore implies the existence of additional new resonances to restore unitarity in WW scattering amplitudes. The new couplings $\kappa_{b,t}$ are related to the width of the scalar into quark pairs,

$$\Gamma_{Sf\bar{f}} = \frac{3\kappa_f^2 m_f^2 M_S}{8\pi v^2} \left(1 - \frac{4m_f^2}{M_S^2}\right)^{3/2} \quad (9)$$

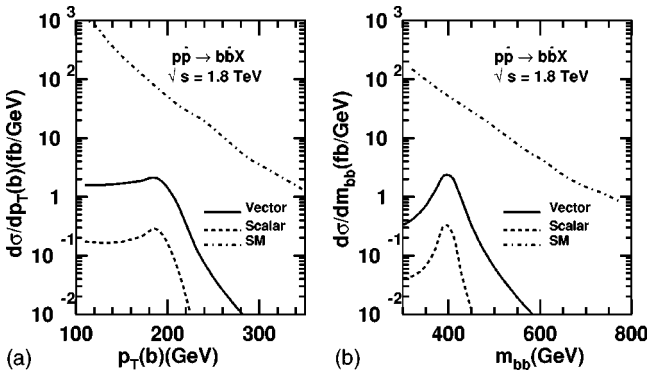


FIG. 2. (a) $p_T(b)$ and (b) $m_{b\bar{b}}$ distributions for the signal and background at the Tevatron. The solid curves correspond to the signal for a vector resonance with $M_V=400$ GeV and $\Gamma_V=47$ GeV. The dashed curves correspond to the signal for a scalar resonance with $M_S=400$ GeV and $\Gamma_S=27$ GeV. The dot-dashed curves are standard model background.

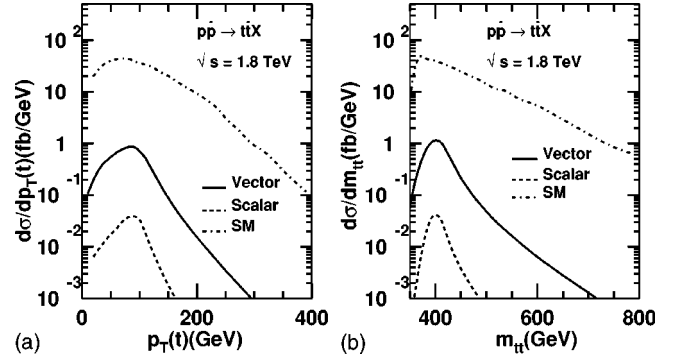


FIG. 3. (a) $p_T(t)$ and (b) $m_{t\bar{t}}$ distributions for the signal and background at the Tevatron. The solid curves correspond to the signal for a vector resonance with $M_V=400$ GeV and $\Gamma_V=47$ GeV. The dashed curves correspond to the signal for a scalar resonance with $M_S=400$ GeV and $\Gamma_S=27$ GeV. The dot-dashed curves are standard model background.

$$\approx 60\kappa_f^2 \left(\frac{m_t}{175 \text{ GeV}}\right)^2 \left(\frac{M_S}{1000 \text{ GeV}}\right) \text{ GeV}, \text{ for } M_S \gg m_f. \quad (10)$$

As argued in Ref. [3] there are few constraints on these couplings from low energy observables. The tightest constraint is obtained by requiring perturbative unitarity [3,8] in the scattering amplitude $b\bar{b}\rightarrow b\bar{b}$ (or in $t\bar{t}\rightarrow t\bar{t}$) through an exchange of the new scalar. This leads to

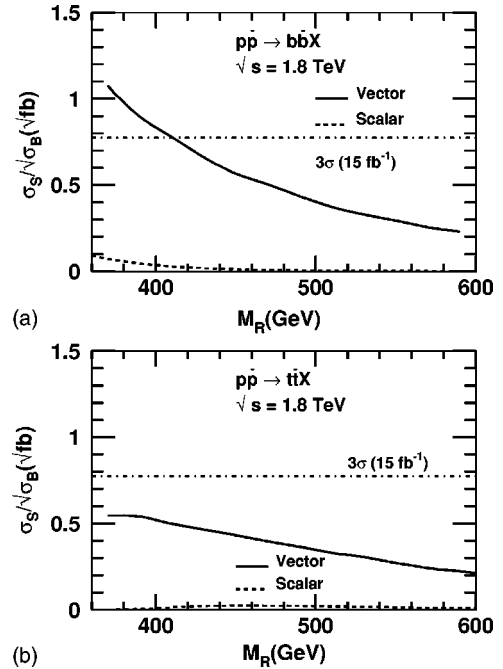


FIG. 4. Statistical sensitivity to a new resonance as a function of the resonance mass for (a) $b\bar{b}$ production, and (b) $t\bar{t}$ production. The solid curve is for a vector resonance and the dotted curve for a scalar resonance. The dot-dashed line indicates the 3σ sensitivity level. We assume a Tevatron Run II integrated luminosity of 15 fb^{-1} .

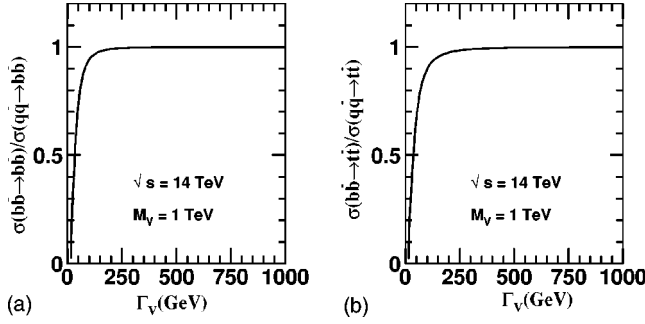


FIG. 5. Relative contribution (a) to $pp \rightarrow b\bar{b}X$ and (b) to $t\bar{t}X$ from $b\bar{b} \rightarrow b\bar{b}$ ($t\bar{t}$) and $q\bar{q} \rightarrow b\bar{b}$ ($t\bar{t}$) processes at the LHC for $M_V = 1$ TeV as a function of Γ_V .

$$\kappa_{b,t} \leq 3. \quad (11)$$

The relative branching fraction for the new scalar resonance decay to $b\bar{b}$ and $t\bar{t}$ pairs is a free parameter depending on the square of the ratio κ_b / κ_t . For our numerical illustrations, we will use

$$\kappa_b = \kappa_t = 1. \quad (12)$$

This appears to be an unusual choice because in many models with couplings such as Eq. (8) one does not have simultaneously large κ_b and κ_t . However, as we will see, different processes that we consider single out one of the couplings. The value we have chosen for these couplings results in an interaction that is weaker than it was in the vector case. A more detailed study would determine the sensitivity to the couplings in both the scalar and vector cases. For $M_S \sim 500$ GeV, $\Gamma(S \rightarrow t\bar{t})$ is only about 36% of $\Gamma(S \rightarrow b\bar{b})$, while for $M_S \sim 1$ TeV, it increases to 82%. Our choice of parameters will allow us to illustrate two slightly different cases: the scalar case will be narrower than the vector case and it will not receive any contribution from light quark annihilation.

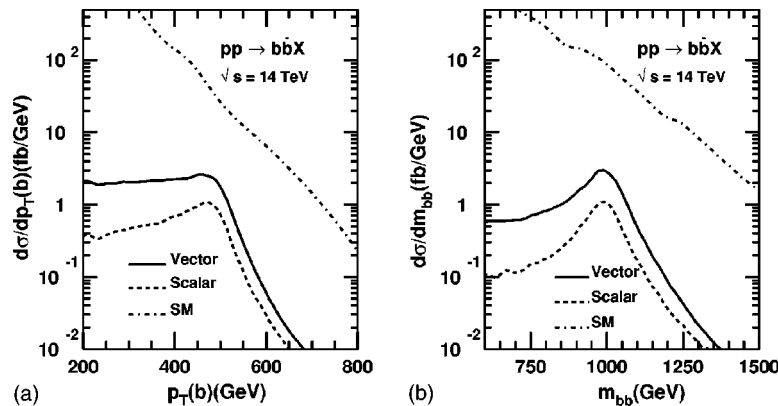


FIG. 6. (a) $p_T(b)$ and (b) $m_{b\bar{b}}$ distributions for the signal and background at the LHC. The signal is calculated for the parameters in Eq. (17) and the dot-dashed curves indicate the standard model background.

III. HEAVY $q\bar{q}$ PAIR PRODUCTION AT THE TEVATRON

The processes $p\bar{p} \rightarrow b\bar{b}X$, $t\bar{t}X$ receive enhanced contributions from the parton level processes $b\bar{b} \rightarrow b\bar{b}$, $t\bar{t}$ involving the s -channel exchange of the new resonance. The vector resonance also receives corrections of electroweak strength from the parton level processes $q\bar{q} \rightarrow b\bar{b}$, $t\bar{t}$ for a light quark q . These contributions can actually be dominant in some regions of parameter space because the light quark content of the proton is much larger than its b content. To the extent that this is possible, we will only consider cases where the $b\bar{b}$ annihilation mechanism dominates to keep our conclusions as model independent as we can.

To this effect we compute the relative contributions of both mechanisms to the processes $p\bar{p} \rightarrow b\bar{b}X$ and $p\bar{p} \rightarrow t\bar{t}X$. We present the results in Figs. 1(a) and 1(b), respectively. We select a resonance mass $M_V = 400$ GeV, which is above threshold for $t\bar{t}$ production and about as large as can be probed by the Tevatron. We present our results as a function of the resonance width Γ_V . Increasing the width corresponds to increasing the coupling to the top and bottom quarks while reducing the coupling to the light quarks. For this reason the fraction of signal events that originates in $b\bar{b}$ annihilation increases as a function of Γ_V . We find that in $b\bar{b}$ production, at $\Gamma_V \geq 45$ GeV, more than 80% of the signal is coming from $b\bar{b}$ annihilation. Since our motivation is to study the couplings to the third generation, we choose $\cot \theta_R = 7$ or $g_V = 0.63$ as in Eq. (6), corresponding to $\Gamma_V \sim 47$ GeV for our Tevatron studies.

For $t\bar{t}$ production on the other hand, light quark annihilation represents a larger fraction of signal events than for $b\bar{b}$ production. Figure 1(b) indicates that $\Gamma_V \geq 100$ GeV would be necessary for $b\bar{b}$ annihilation to produce 50% of the signal, and about $\Gamma_V \geq 200$ GeV for it to dominate. These values, however, correspond to unacceptably large couplings. We thus keep $\Gamma_V \sim 47$ GeV. In this case only 17% of the signal events are produced through the couplings that we want to study. We will be able to improve this situation with the higher energy available at the LHC.

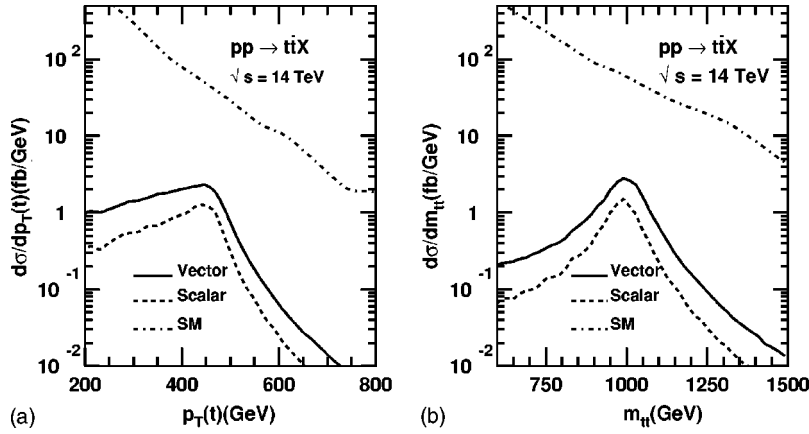


FIG. 7. (a) $p_T(t)$ and (b) $m_{t\bar{t}}$ distributions for the signal and background at the LHC. For the signal we use the parameters of Eq. (17) and the dot-dashed curves indicate the standard model background.

For the scalar resonance the signal arises exclusively from $b\bar{b}$ annihilation for both $b\bar{b}$ and $t\bar{t}$ production because we are ignoring the couplings to the light quarks. It is evident that $b\bar{b}$ production will only be sensitive to κ_b , whereas $t\bar{t}$ production will be sensitive to the product $\kappa_b\kappa_t$. As we mentioned in the Introduction, many scalars found in models commonly discussed have enhanced couplings to b or t quarks but not to both at the same time. For those cases we would not expect a signal in $t\bar{t}$ production. For illustration we choose $\kappa_b = \kappa_t = 1$, as in Eq. (12), well below the unitar-

ity constraint. For a 400 GeV scalar mass this then corresponds to $\Gamma_S = 27$ GeV. With these parameters, our scalar resonance is roughly half as narrow as our vector resonance and we expect relatively fewer signal events.

We first consider $b\bar{b}$ production and demand both b 's to be tagged. We assume a combined efficiency of 50% (or about 70% for each tagged b) [9]. We compute the standard model background with the aid of MADGRAPH [10]. We include both the physical background consisting of QCD produced $b\bar{b}$ pairs, as well as a fake background that results when final state light quarks mimic a $b\bar{b}$ pair. The rate at which this occurs is assumed to be 0.5% [9]. The main production mechanism for the background $b\bar{b}$ pairs at the Tevatron is the QCD process via gluon fusion. The background $b\bar{b}$ pairs have mostly low or intermediate transverse momentum and we adopt a p_T cut to suppress them. We also adopt a rapidity cut that mimics the typical coverage of D0 and CDF Fermilab detectors. Our basic cuts for Tevatron processes will thus be

$$p_T(b) > 100 \text{ GeV}, \quad |y_b| < 2. \quad (13)$$

We show the transverse momentum $p_T(b)$ and the invariant mass $m_{b\bar{b}}$ distributions in Figs. 2(a) and 2(b) respectively. Unfortunately the background is several orders of magnitude larger than the signal and we were not able to find a way to reduce it significantly while preserving the signal. To compute the statistical sensitivity of this process we optimize the signal/background ratio with the cut that discards events more than two widths away from the resonance mass,

$$M_R - 2\Gamma_R < m_{b\bar{b}} < M_R + 2\Gamma_R. \quad (14)$$

We now turn our attention to $t\bar{t}$ production. As was the case with $b\bar{b}$ production, the main background is QCD production of $t\bar{t}$ pairs. In this case the background is also two orders of magnitude larger than the signal. In Fig. 3, we show the top transverse momentum $p_T(t)$ and invariant mass $m_{t\bar{t}}$ distributions for both signal and background. For the signal we use the same model parameters we used in $b\bar{b}$ production. We also implement the kinematical cut

$$|y_t| < 2. \quad (15)$$

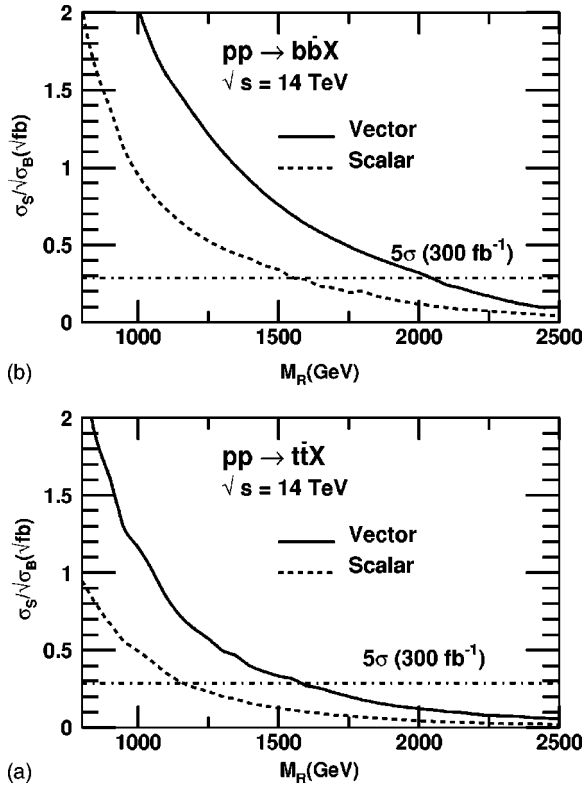


FIG. 8. Statistical sensitivity at the LHC with an integrated luminosity of 300 fb^{-1} to a new resonance as a function of the resonance mass for (a) $b\bar{b}$ production, and (b) $t\bar{t}$ production. The solid curve is for a vector resonance and the dotted curve for a scalar resonance. The dot-dashed line indicates the 5σ sensitivity level. The couplings have been taken as in Eq. (17).

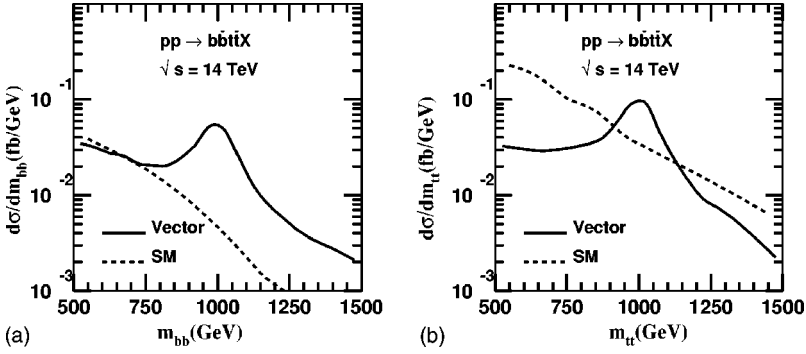


FIG. 9. (a) $m_{b\bar{b}}$ and (b) $m_{t\bar{t}}$ distributions for a vector resonance with $M_V=1$ TeV and $\Gamma_V=127$ GeV (solid curves) and the SM background (dashed curves) in $pp\rightarrow b\bar{b}t\bar{t}X$ at the LHC.

Once again we optimize the sensitivity to new physics by selecting the $m_{t\bar{t}}$ invariant mass region around the resonance as per Eq. (14).

We estimate the statistical sensitivity to the signal by simply dividing the number of signal events by the square root of the number of the background events:

$$\frac{\sigma_S}{\sqrt{\sigma_B}}\sqrt{L}, \quad (16)$$

where L is the total integrated luminosity. We show this statistical sensitivity for the Tevatron Run II as a function of the resonance mass in Fig. 4. To obtain our numbers we are using semileptonic channels for signal identification. One of the t quarks decays leptonically into an electron or a muon and the other one decays hadronically. With 50% $b\bar{b}$ -tagging efficiency we end up using a combined event efficiency of about 16%. The dot-dashed line in the figure indicates the 3σ signal sensitivity assuming a total integrated luminosity of 15 fb^{-1} . This figure indicates that it might be possible to observe a 3σ signal for a resonance lighter than about $M_R < 400$ GeV in $b\bar{b}$ production. However, given the very low signal to background ratio more realistic studies at the detector level would be needed to conclude that this is observable at the Tevatron. We also conclude that the Tevatron is not sensitive to this type of new physics through the $t\bar{t}$ channel. In all cases we used couplings given by Eqs. (6) and (12) and we do not expect the conclusions to change if we choose the model parameters differently. The better sensitivity to a vector resonance is in large part due to its additional production mechanism through light quark annihilation. As mentioned in the Introduction these couplings to light quarks are very model dependent.

IV. SIGNALS AT THE LHC

The higher energy of the LHC allows us to consider different types of signals in this case. We begin with the heavy-quark pair production processes at the Tevatron. We then discuss associated production of the new resonance with both heavy quark pair $b\bar{b}$, $t\bar{t}$ [11], and a single top [12]. Although both of these processes have significantly smaller cross sections than the Drell-Yan type of heavy-quark pair signal, they also have much smaller backgrounds and a unique topology that offers a better chance for the signal observation.

A. $pp\rightarrow b\bar{b}X$ and $t\bar{t}X$

The rates for the processes $pp\rightarrow b\bar{b}X$, $t\bar{t}X$ are much larger at the higher center of mass energies that can be reached at the LHC. It is also possible to search for heavier resonances for which the signal/background ratio is expected to be larger than what was possible at the Tevatron. We first explore the vector resonance. In Fig. 5, we show the relative contributions to the signal from the $b\bar{b}$ annihilation process for $M_V=1$ TeV as a function of Γ_V . We see that for both final states about 85% of the signal events originate from $b\bar{b}$ annihilation if Γ_V is larger than 60 GeV. In this case we are much less sensitive to the more model-dependent terms that arise from the light-quark annihilation processes. For illustration, we keep the same couplings that were used for the Tevatron studies in the last section: $g_V=0.63$ for the vector and $\kappa_b=\kappa_t=1$ for the scalar, as given in Eqs. (6) and (12). The signal parameters we use for the LHC are thus

$$M_R=1 \text{ TeV}, \Gamma_V=127 \text{ GeV}, \Gamma_S=110 \text{ GeV}. \quad (17)$$

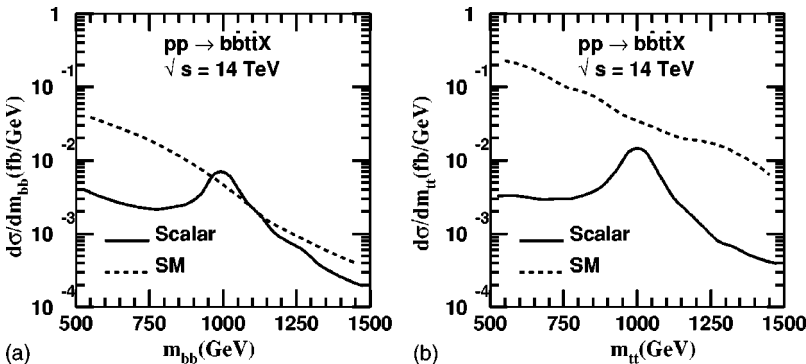


FIG. 10. (a) $m_{b\bar{b}}$ and (b) $m_{t\bar{t}}$ distributions for a scalar resonance with $M_S=1$ TeV and $\Gamma_S=110$ GeV (solid curves) and the SM background (dashed curves) in $pp\rightarrow b\bar{b}t\bar{t}X$ at the LHC.

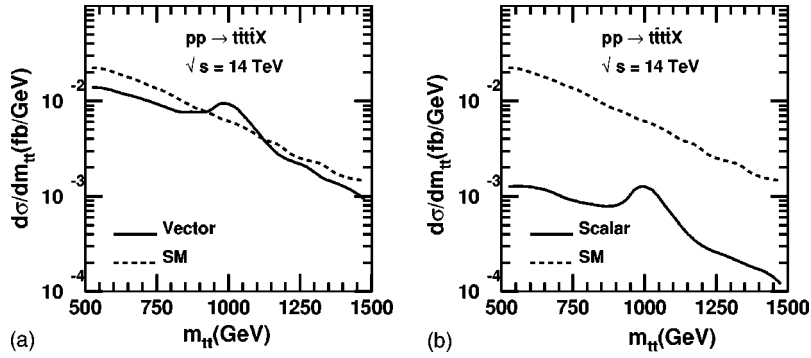


FIG. 11. m_{tt} distributions for $pp \rightarrow t\bar{t}\bar{t}X$ at the LHC for (a) a vector resonance and (b) a scalar resonance with the parameters of Eq. (17). The SM background is depicted by the dashed curve.

For the processes $pp \rightarrow b\bar{b}X, t\bar{t}X$ at the LHC we evaluate both the signal and background with the basic cuts

$$p_T(b,t) > 200 \text{ GeV}, \quad |y_{b,t}| < 2, \quad (18)$$

as well as with the cuts of Eq. (14) to optimize the signal/background ratio. In Fig. 6 we show the $p_T(b)$ and $m_{b\bar{b}}$ distributions for $pp \rightarrow b\bar{b}X$. The corresponding distributions for $pp \rightarrow t\bar{t}X$ are presented in Fig. 7. We see from these figures that the background at the LHC is about one order of magnitude larger than the signal. This is already better than the situation for the lower resonance mass at the Tevatron. The statistical sensitivity for the signals at the LHC is summarized in Fig. 8. We have used the same tagging rates and efficiencies as in the Tevatron. The dot-dashed lines indicate

the 5σ sensitivity assuming a total integrated luminosity of 300 fb^{-1} . The figure shows that the sensitivity extends to about $M_R \approx 2 \text{ TeV}$ at a 5σ level, for both vector and scalar signals and for both $b\bar{b}$ and $t\bar{t}$ channels. Although the situation looks much more promising than at the Tevatron, due to the much larger luminosity and production cross section, we must still bear in mind that the signal/background ratio is small and that more realistic simulations including detector effects are necessary to reach definitive conclusions.

B. $pp \rightarrow b\bar{b}t\bar{t}X$

The much larger phase space available at the LHC permits us to explore more complicated processes. In particular, processes with four heavy quarks, originating in the production of the heavy resonance in association with two heavy quarks, have been found to be very useful in Higgs studies [11]. At LHC energies these processes would be dominated by the initial subprocess $gg \rightarrow b\bar{b}$ followed by a heavy resonance radiated off one of the b quarks. Since this coupling is enhanced in the new physics scenario that we are considering, this process could be significantly large. In addition, its unique topology could make the large QCD backgrounds more manageable. In this section we investigate this possibility. We use the program COMPHEP [13] to compute the signal cross sections for this process.

In the process $pp \rightarrow b\bar{b}t\bar{t}X$ one of the b quarks radiates a heavy resonance that decays to $t\bar{t}$. There is also a contribution from $gg \rightarrow t\bar{t}R$ followed by a decay $R \rightarrow b\bar{b}$. The signal is completely dominated by the gluon fusion process. There is also a much smaller contribution initiated by $b\bar{b}$ annihilation that we have calculated but not included. For illustration we use the same model parameters as in the preceding section, Eq. (17). We implement basic cuts

$$p_T(b) > 100 \text{ GeV}, \quad p_T(t) > 50 \text{ GeV}, \quad |y_b| < 2. \quad (19)$$

In Figs. 9 and 10, we show the $m_{b\bar{b}}$ and $m_{t\bar{t}}$ distributions for the process $pp \rightarrow b\bar{b}t\bar{t}X$ at the LHC for a vector and a scalar resonances, respectively. As expected, there are peaks in these distributions originating in the resonance. It is particularly encouraging to see that the signal peaks are above the continuum background, making a signal observation more promising than in the channels studied in the preceding sections. With the parameters we have chosen, the vector reso-

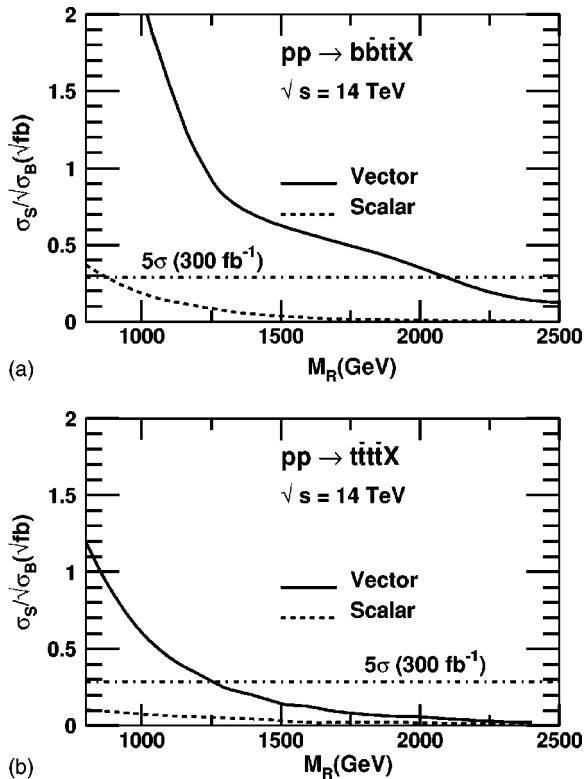


FIG. 12. Statistical sensitivity at the LHC with an integrated luminosity of 300 fb^{-1} to a new resonance as a function of the resonance mass for (a) $pp \rightarrow b\bar{b}t\bar{t}X$, and (b) $pp \rightarrow t\bar{t}\bar{t}X$. We use the parameters given in Eq. (17).

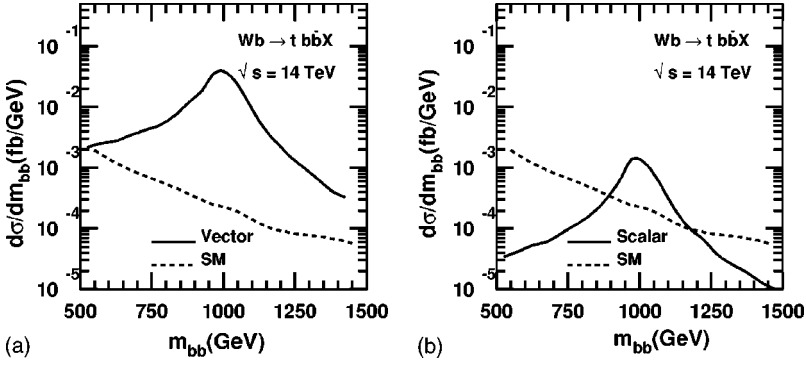


FIG. 13. $m_{b\bar{b}}$ distributions in $Wb \rightarrow t b \bar{b} X$ at the LHC for (a) a vector resonance and for (b) a scalar resonance with the parameters of Eq. (17). The SM background is indicated by the dashed curve.

nance has a larger production rate than the scalar resonance and therefore results in a larger reach for the LHC. This, however, mostly reflects the fact that we have chosen somewhat weaker couplings for the scalar resonance. An additional cut is used to optimize the signal/background ratio,

$$M_R - 4\Gamma_R < m_{b\bar{b}, t\bar{t}} < M_R + 4\Gamma_R. \quad (20)$$

Applying this cut to both $m_{b\bar{b}}$ and $m_{t\bar{t}}$, we present the sensitivity at the LHC assuming a total integrated luminosity of 300 fb^{-1} in Fig. 12. We have used the same identification efficiencies for the b and t quarks as before. We see that a 5σ sensitivity may be reached for masses up to 2 TeV for the vector resonance.

C. $pp \rightarrow t\bar{t} X$

The heavy resonance can also be produced in association with a $t\bar{t}$ pair. The dominant production mechanism for this mode is again gluon fusion. We have also calculated the $b\bar{b}$ annihilation mechanism but found it to be two orders of magnitude smaller and do not include it. We compute our signals with the program COMPHEP [13]. Figure 11 shows the $m_{t\bar{t}}$ distributions for new resonances with the same parameters as in Eq. (17). For the new scalar this channel is sensitive to κ_t^2 , whereas the $pp \rightarrow b\bar{b} t\bar{t} X$ channel is sensitive to $\kappa_t \kappa_b$. This distinction is important in models where only one of these couplings is large. We use the same basic cuts as in Eq. (19). To construct the $m_{t\bar{t}}$ variable we have selected one t and one \bar{t} randomly. We therefore assume that it is possible to distinguish the t from the \bar{t} via their leptonic decays. Using Eq. (20), we present the statistical sensitivity of this pro-

cess in Fig. 12 using 16% event efficiency for *each* $t\bar{t}$ pair. Due to the lower cross section and identification efficiency the reach in this channel is somewhat smaller than in the $pp \rightarrow b\bar{b} t\bar{t} X$ channel.

D. $Wb \rightarrow t, b\bar{b}; t, \bar{t}$

It is well known that single top quark production via the electroweak process $Wb \rightarrow t$ can be sizable due to the enhanced longitudinal gauge boson coupling $W_L t b$ at high energies [12]. The cross section for single top production increases with energy up to about one-third of the cross section for $t\bar{t}$ pair production [14]. The main advantage of this channel is the substantially smaller standard model background. We now consider the effect of our new resonances on this process using the program COMPHEP [13] to compute the signals. For this case only, we also use COMPHEP to estimate the standard model background.

We first consider the $Wb \rightarrow t b \bar{b}$ process with the basic cuts

$$p_T(t, b) > 100 \text{ GeV}, \quad |y_{t, b}| < 2. \quad (21)$$

The high p_T cut is imposed on *all* heavy quarks, including the two b quarks that reconstruct the resonance mass as well as the single top quark.

In Fig. 13, we show the $m_{b\bar{b}}$ distribution. We see that the signals can be significantly above the SM background in this case. We use the cuts of Eq. (20) to estimate the sensitivity to the new physics.

For the process $Wb \rightarrow t\bar{t}$ the standard model background is even smaller. The basic cut $|y_t| < 2$ leads us to the results

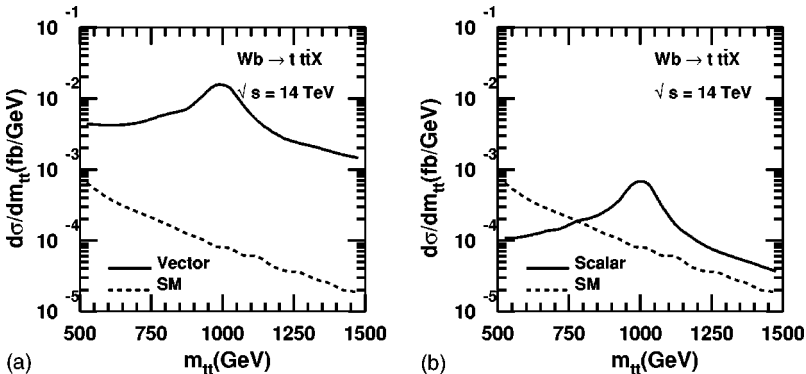


FIG. 14. $m_{t\bar{t}}$ distribution in the process $Wb \rightarrow t\bar{t} X$ at the LHC for (a) a vector resonance and for (b) a scalar resonance with parameters given in Eq. (17). The SM background is indicated by the dashed line.

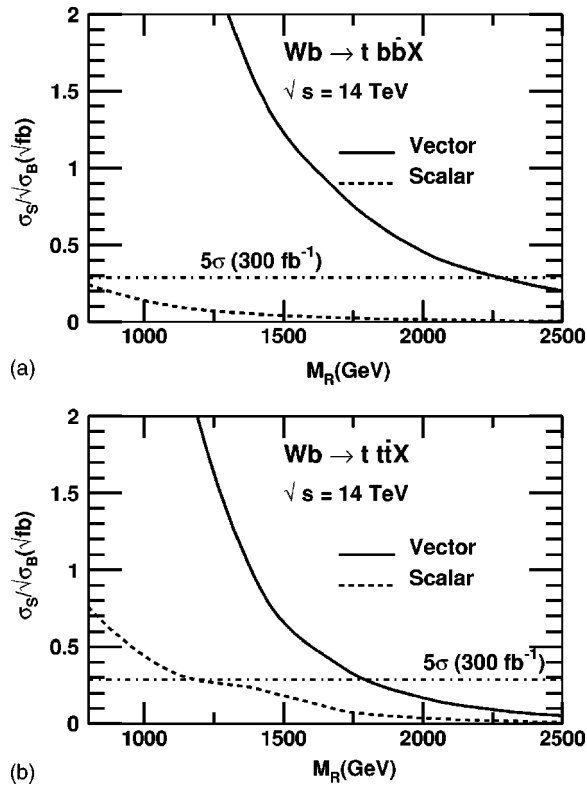


FIG. 15. Statistical sensitivity at the LHC with an integrated luminosity of 300 fb^{-1} to a new resonance as a function of the resonance mass through the processes (a) $Wb \rightarrow t b \bar{b} X$, and (b) $Wb \rightarrow t t \bar{t} X$. The solid curve is for a vector resonance and the dotted curve for a scalar resonance with parameters as in Eq. (17). The dot-dashed line indicates the 5σ sensitivity level.

in Fig. 14. This process has the largest signal/background ratio of all the ones we have considered. Using the same b and t efficiencies that we used for the Tevatron, we show in Fig. 15 the reach in this case.

V. CONCLUSION

We have presented a preliminary study of signals for new resonances coupling to heavy quarks at the Tevatron and the

LHC. We have considered a scalar and a vector resonance with masses of 400 GeV for the Tevatron study and 1 TeV for the LHC study and we have chosen couplings so that the resonances couple strongly to the top quark but are sufficiently narrow to be described by a Breit-Wigner shape. These parameters satisfy the existing constraints.

The most direct production mechanism is the Drell-Yan process for $pp \rightarrow b \bar{b} X$ and $t \bar{t} X$. At the Tevatron, due to the rather low production rate and substantial background from the heavy quark production, only a weak 3σ bound may be put on the vector state signal for $M_V < 400$ GeV.

At the LHC, on the other hand, the situation can be significantly improved. A 5σ statistical sensitivity may be reached for both a vector and a scalar state with $M_R \sim 1.5$ TeV. However, the large QCD backgrounds for the heavy quark pair production still lead to a low signal-to-background ratio (less than 10%) near the resonance peaks. This renders the signal observation systematically difficult.

We found that the most promising channels for the signal searches are multiple heavy quark production. The first class of processes is essentially due to the $gg \rightarrow b \bar{b}, t \bar{t}$ with a heavy resonance radiation off a heavy quark leg. Consequently, the 4-quark signals $b \bar{b} t \bar{t}$ and $t \bar{t} t \bar{t}$ would have much less severe SM backgrounds. It is very interesting to note that the electroweak process $Wb \rightarrow t$, again associated with a heavy resonance radiation off the top quark, could lead to very strong signal as well. The reach can be up to $M_V \sim 2$ TeV with a 5σ significance. More detailed studies including detector issues would be needed to reach more definitive conclusions and to fully determine the range of parameters that can be probed by the LHC.

ACKNOWLEDGMENT

The work of T.H. was supported in part by the U.S. DOE under Contract No. DE-FG02-95ER40896, in part by the Wisconsin Alumni Research Foundation, and in part by National Natural Science Foundation of China. The work of G.V. and Y. W. was supported in part by DOE under contact number DE-FG02-01ER41155.

-
- [1] M.S. Chanowitz, Phys. Rev. Lett. **87**, 231802 (2001); M.S. Chanowitz, Phys. Rev. D **66**, 073002 (2002).
 [2] C.T. Hill, Phys. Lett. B **266**, 419 (1991); **345**, 483 (1995); E. Eichten and K. Lane, *ibid.* **352**, 382 (1995).
 [3] T. Han, Y.J. Kim, A. Likhoded, and G. Valencia, Nucl. Phys. **B593**, 415 (2001); T. Han, D. Rainwater, and G. Valencia, Phys. Rev. D **68**, 015003 (2003).
 [4] X.G. He and G. Valencia, Phys. Rev. D **66**, 013004 (2002); **66**, 079901(E) (2002); **68**, 033011 (2003); hep-ph/0404229.
 [5] S. Dawson and G. Valencia, Nucl. Phys. **B348**, 23 (1991); R.D. Peccei, S. Peris, and X. Zhang, *ibid.* **B349**, 305 (1991); S. Dawson and G. Valencia, Phys. Rev. D **53**, 1721 (1996); F. Larios and C.P. Yuan, *ibid.* **55**, 7218 (1997); F. Larios, M.A. Perez, and C.P. Yuan, Phys. Lett. B **457**, 334 (1999).
 [6] C.T. Hill and S.J. Parke, Phys. Rev. D **49**, 4454 (1994).
 [7] R. Casalbuoni *et al.*, Phys. Lett. **155B**, 95 (1985); Nucl. Phys. **B282**, 235 (1987); **B310**, 181 (1988); Phys. Lett. B **249**, 130 (1990); **253**, 275 (1991).
 [8] B.W. Lee, C. Quigg, and H.B. Thacker, Phys. Rev. D **16**, 1519 (1977); M.S. Chanowitz, M.A. Furman, and I. Hinchliffe, Nucl. Phys. **B153**, 402 (1979); T. Appelquist and M.S. Chanowitz, Phys. Rev. Lett. **59**, 2405 (1987); **60**, 1589(E) (1988); W.J. Marciano, G. Valencia, and S. Willenbrock, Phys. Rev. D **40**, 1725 (1989); S. Jager and S. Willenbrock, Phys. Lett. B **435**, 139 (1998).

- [9] Elizaveta Chabalina (private communication).
- [10] T. Stelzer and W.F. Long, *Comput. Phys. Commun.* **81**, 357 (1994).
- [11] Z. Kunszt, *Nucl. Phys.* **B247**, 339 (1984); W.J. Marciano and F.E. Paige, *Phys. Rev. Lett.* **66**, 2433 (1991); J.F. Gunion, *Phys. Lett. B* **261**, 510 (1991).
- [12] S.S.D. Willenbrock and D.A. Dicus, *Phys. Rev. D* **34**, 155 (1986); C.P. Yuan, *ibid.* **41**, 42 (1990); S. Cortese, and R. Petronzio, *Phys. Lett. B* **253**, 494 (1991); R.K. Ellis and S. Parke, *Phys. Rev. D* **46**, 3785 (1992); F. Maltoni, K. Paul, T. Stelzer, and S. Willenbrock, *ibid.* **64**, 094023 (2001); T. Tait and C.P. Yuan, *ibid.* **63**, 014018 (2001); E. Boos, L. Dudko, and T. Ohl, *Eur. Phys. J. C* **11**, 473 (1999).
- [13] A. Pukhov *et al.*, hep-ph/9908288.
- [14] T. Stelzer, Z. Sullivan, and S. Willenbrock, *Phys. Rev. D* **58**, 094021 (1998); M. Beneke *et al.*, in Proceedings of the Workshop on Standard Model Physics (and more) at the LHC; M. Beneke *et al.*, hep-ph/0003033.